Cooperation Scenarios in Cooperative Multiple Access Channels

Paul Ferrand, Claire Goursaud, Jean-Marie Gorce

Cooperation Scenarios in Cooperative Multiple Access Channels

Paul Ferrand, Claire Goursaud and Jean-Marie Gorce
Université de Lyon, INRIA
INSA-Lyon, CITI, F-69621, France
Tel : +334-72437322
E-mail: name.surname@insa-lyon.fr

***Abstract*—In this paper, we present preliminary results on achievables rates in half-duplex cooperative multiple access channels (CMAC). We show that the upper bound on the capacity of the half-duplex CMAC can be solved using convex optimization techniques. Under a Gaussian model, we study the maximal achievable rate by every node in the network. We propose a number of scenarios, encompassing existing and theoretical cooperation schemes. Using these hypotheses, we evaluate the performance of both a non-cooperative concurrent access and simple cooperative multi-hop or relaying schemes with respect to the upper bound. The performance is compared for the various scenarios, and we provide analyses of specific cases in order to illustrate how our framework may be used to answer targeted questions about the capacity of CMACs.**

I. Introduction

For more than two decades, the growth of mobile communications led to a renewed interest on the capacity of wireless channels and networks. While the basis of the studies are still the same when compared to classical communication theory, general results have to take into account the strong constraint that nodes can not send and receive information at the same time. Kramer [1] and Khojastepour *et al.* [2] provide straightforward ways to extend the classical capacity theorems to multi-states channels, a general model encompassing half-duplex networks.

Among half-duplex networks, we focus our study in this paper onto 3-nodes networks. The most classical of such models is the relay channel, where a node transmits information to a destination with the help of the other node. In [3], the upper bound on the capacity of the channel is given, along with the now classical decode-and-forward and compress-and-forward lower bounds. Optimizing the capacity of the relay channel under a total power constraint has been the topic of [4], where the authors developed an algorithm akin to waterfilling for the power allocation, for both the half and full duplex relay channel. In [5], the capacity of the coherent full-duplex relay channel is given under different CSI and power allocation schemes. In [6], the authors proposed an adaptative partial decode-and-forward lower bound, and gave results for the optimal power allocation based on fixed-point algorithms.

Another scheme to consider for the 3-nodes network is the multiple access scheme, where two nodes act as information sources. The capacity of the multiple access channel (MAC) is known in the general case, and can be found in [7]. However, the capacity of the cooperative MAC, where both nodes may help each other in transmitting information to the destination, is still an open problem. This model has been studied by Laneman in his thesis [8], where he gave both an upper-bound and a decode and forward lower-bound on the capacity of the full-duplex CMAC. Sendonaris *et al.* studied this channel extensively in [9], and designed a realistic and usable decode-and-forward scheme, along with its implementation. Their study used full-duplex results but in CDMA orthogonal sub-channels. More recently, Mesbah and Davidson gave an optimal power allocation for the same protocol Sendonaris *et al.* described [10]. They also showed that a more general half-duplex version was able to be solved as a quasiconvex problem, using bisection methods.

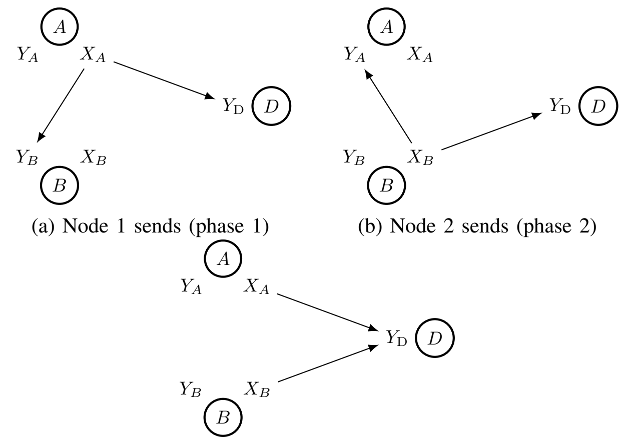

(a) Node 1 sends (phase 1) (b) Node 2 sends (phase 2)

(c) Cooperating phase (phase 3)

Fig. 1. The half-duplex cooperative multiple access channel. The channel is at each time in one of the 3 phases presented here.

In this paper, we iterate on previous work [11], using these results to answer target questions about the capacity of Gaussians CMACs. We define a number of realistic scenarii and cast them as constraints in our problem, and subsequently analyze the effect of the new constraints on the capacity region in Sec.IV-A. We evaluate whether it is interesting to implement beamforming when using alternating relay channels in Sec.IV-B. Finally we study the impact of a maximum transmission power constraint and show it does affect the achievable rate if the constraint is too low (Sec. IV-C).

$$R_A \leq \tau_1 \log\left(1 + (|h_{A,B}|^2 + |h_{A,D}|^2) P_A^{(1)}\right) + \tau_3 \log\left(1 + |h_{A,D}|^2 (1-\rho^2) P_A^{(3)})\right) \quad \text{(1a)}$$

$$R_A \leq \tau_2 \log\left(1 + (|h_{A,B}|^2 + |h_{A,D}|^2) P_B^{(2)}\right) + \tau_3 \log\left(1 + |h_{B,D}|^2 (1-\rho^2) P_B^{(3)})\right) \quad \text{(1b)}$$

$$R_A + R_B \leq \tau_1 \log\left(1 + |h_{A,D}|^2 P_A^{(1)}\right) + \tau_2 \log\left(1 + |h_{B,D}|^2 P_B^{(2)}\right) \quad \text{(1c)}$$

$$+ \tau_3 \log\left(1 + |h_{A,D}|^2 P_A^{(3)} + |h_{B,D}|^2 P_B^{(3)} + 2\rho |h_{A,D}||h_{B,D}| \sqrt{P_A^{(3)} P_B^{(3)}}\right)$$

II. Model description

A. Network and channel model

Our base model is a half-duplex cooperative multiple access channel (HD-CMAC), composed of two source nodes and a destination node. Each source aims at transmitting its own message, possibly helping the other along the way. The half-duplex constraint implies that the nodes may not send and receive at the same time. We write X_i and Y_i the signal sent and received by the node $i \in \{A, B\}$, while the message received by the destination is Y_D.

From [2] we can write the upper bound on the capacity of this channel as the capacity of every cut in the network across all the possible states and their associated time-share in the schedule. We consider that the network spends a fraction τ_j of its global time in one of the corresponding phase j represented on Fig.1, with $j \in \{1, \ldots, 3\}$. We focus on this paper on an analysis of the Gaussian channel. We can thereby derive the outer bound in a classical manner, as can be seen in [2], [7]. We consider that nodes are subjected to some power allocation, where for each phase j each node i uses $\mathbf{P}_i^{(j)}$ power for transmitting its signal. Furthermore, the channel coefficient $h_{i,k}$ between nodes i and $k \in \{A, B, D\}$ is stable and symmetrical. Each node is subject to a Gaussian white noise of density N_0 at its receiver. We can thus use the normalized power – w.r.t. the noise density – $P_i^{(j)} = \mathbf{P}_i^{(j)}/N_0$ as the power value in any equation. The signals from the source nodes to the destination have a potential correlation factor ρ. This correlation stems from their cooperation, and requires a coherent transmission between both sources on top of a joint codebook design for the cooperative phase. We consider natural logarithms and our capacity results are thus in nats/s.

The upper bound on the capacity of this channel can be written as the convex closure of all (R_A, R_B) verifying (1), where R_1 and R_B are the rates of sources A and B respectively. The region changes for different values of the time-sharing vector $\mathbf{t} = (\tau_1, \tau_2, \tau_3)$ and the power-sharing vector $\mathbf{P} = (P_A^{(1)}, P_B^{(2)}, P_A^{(3)}, P_B^{(3)})$, which are the values to be optimized. In order to simplify the expression, we decide to normalize the power further by the value of the channel coefficient of the inter-source link $h_{A,B}$, e.g. changing $P_i^{(j)}$ into $\bar{P}_i^{(j)} = |h_{A,B}|^2 P_i^{(j)}$. This leads us not to consider the A-D link and B-D link channel coefficients directly, but rather their relative quality w.r.t. to the inter-source link. We will write $l_1 = h_{A,D}^2 / h_{A,B}^2$ and $l_2 = h_{B,D}^2 / h_{A,B}^2$ in the remainder of the paper.

B. Common rate

Unlike the single link case, there are no unilateraly *best achievable region* in a multi-source channel model. We may well have a better achievable rate for the second source, at the expense of the rate of the first source. A common criteria in the study of multi-source networks is thus the sum of the rates of the nodes, but we propose here to study the maximal rate every node may attain simultaneously. This can be understood as a quality of service constraint on the nodes. In our model, the common rate semi-line $R_A = R_B = R$ will intersect the convex closure of every possible rate regions obtained using (1) at a single point in realistic cases, allowing us to go from treating a region of achievable rates to a single rate variable R.

III. The upper and lower bound optimization problems

In this section, we describe how to transform the upper bound in (1) into a convex optimization problem. We will use the standard form of such problems, which are described as the minimization of a convex function $f_0(\mathbf{x})$ of $\mathbf{x} \in \mathbb{R}^n$ subject to some inequalities $f_i(\mathbf{x}) \leq 0$, where the functions f_i are convex in $\mathbf{x}$, and equalities of the form $h_j(\mathbf{x}) = 0$, where h_j are linear functions of $\mathbf{x}$ [12]. Expressing our problems as convex optimization problems allows for very quick numerical evaluation, using methods like sequential quadratic programming [13] or modified interior-point methods [12] which are readily implemented in most numerical computation softwares. In fact, an optimal solution obtained with any method is certified to be the global optimal solution since our problems are transformed into convex ones. While we discuss these transformations in [11], we only state the general result here and use it as is in the last section of this paper.

A. Upper bound on the capacity of the CMAC

We wish to maximize the common rate R, as defined in Sec.II-B, under the constraints defined in (1). Our objective is $-R$, a linear and thus convex function of R. We define the energy variables for node i in slot j as $E_i^{(j)}$. The rationale behind this change and the following one is explained in [11]. We also define an energy-sharing vector α dividing the total energy E_{tot} as:

$$\beta^T E_{\text{tot}} = (\bar{E}_1^{(1)}, \bar{E}_2^{(2)}, \bar{E}_1^{(3)}, \bar{E}_2^{(3)}) \quad \mathbb{1}^T \beta = 1 \quad (3)$$

$$f_1(\tau,\beta,\mathbf{u}) = \tau_1 \log\left(1+(1+l_1)\frac{\beta_1}{\tau_1}E_{\text{tot}}\right) + \tau_3 \log\left(1+l_1\frac{u_1}{\tau_3}E_{\text{tot}}\right) \tag{2a}$$

$$f_2(\tau,\beta,\mathbf{u}) = \tau_2 \log\left(1+(1+l_2)\frac{\beta_2}{\tau_2}E_{\text{tot}}\right) + \tau_3 \log\left(1+l_1\frac{u_2}{\tau_3}E_{\text{tot}}\right) \tag{2b}$$

$$f_3(\tau,\beta,\mathbf{u}) = \tau_1 \log\left(1+l_1\frac{\beta_1}{\tau_1}E_{\text{tot}}\right) + \tau_2 \log\left(1+l_2\frac{\beta_2}{\tau_2}E_{\text{tot}}\right) + \tau_3 \log\left(1+\left(l_1\beta_3+l_2\beta_4+2\sqrt{l_1l_2\beta_4u_3}\right)\frac{E_{\text{tot}}}{\tau_3}\right) \tag{2c}$$

$$f_4(\tau,\beta,\mathbf{u}) = \tau_1 \log\left(1+l_1\frac{\beta_1}{\tau_1}E_{\text{tot}}\right) + \tau_2 \log\left(1+l_2\frac{\beta_2}{\tau_2}E_{\text{tot}}\right) + \tau_3 \log\left(1+\left(l_1\beta_3+l_2\beta_4+2\sqrt{l_1l_2\beta_3u_4}\right)\frac{E_{\text{tot}}}{\tau_3}\right) \tag{2d}$$

We also introduce new variables $\rho_1 = 1-\rho^2$ and $\rho_2 = \rho^2$, further used to form the variables u_i combined in a vector $\mathbf{u} = (\beta_3\rho_1, \beta_4\rho_1, \beta_3\rho_2, \beta_4\rho_2)$. We can formulate the upper bound as a convex optimization problem:

$$\begin{array}{ll} \underset{\tau,\beta,\mathbf{u},R}{\text{minimize}} & -R \\ \text{subject to} & R \le f_1(\tau,\beta,\mathbf{u}) \\ & R \le f_2(\tau,\beta,\mathbf{u}) \\ & 2R \le f_3(\tau,\beta,\mathbf{u}) \\ & 2R \le f_4(\tau,\beta,\mathbf{u}) \\ & \mathbb{1}^T\tau = 1 \\ & \mathbb{1}^T\beta = 1 \\ & u_1+u_3 = \beta_3 \\ & u_2+u_4=\beta_4 \end{array} \tag{4}$$

We note $\mathbb{1}$ a vector of 1, and the functions f_i are written in (2) at the top of the page. In the following sections and results, we will consider both the *coherent* and *non-coherent* case for the capacity of the CMAC. In the *non-coherent* case the correlation parameter ρ in (1) is set equal to 0. In realistic systems, two conditions have to be met in order to have a non-zero correlation parameter ; the nodes must be able to create a joint codebook so that the symbols they send add in a constructive manner, and the transmitted waveforms have to add coherently at the destination. In half-duplex networks, the former condition is easier to achieve than the latter, since there's an exchange of information before the common transmission phase in every case.

B. Lower bounds on the capacity of the CMAC

We will compare two lower bounds with this upper bound. The non-cooperative multiple access capacity is known in general, and is attainable through a combination of superposition coding, successive cancellation decoding and time-sharing [7, ch.8]. Since the medium access is concurrent, there is no time-sharing vector in this lower bound, but an energy-sharing vector $\gamma = (\gamma_1, \gamma_2)$. We have:

$$R \le \log(1+l_1\gamma_1E_{\text{tot}}) \tag{5a}$$

$$R \le \log(1+l_2\gamma_2E_{\text{tot}}) \tag{5b}$$

$$2R \le \log(1+l_1\gamma_1E_{\text{tot}}+l_2\gamma_2E_{\text{tot}}) \tag{5c}$$

These functions are convex in γ_1 and γ_2, and thus we can write an optimization problem similar to (4) with the constraint $\gamma_1+\gamma_2 = 1$. We call this scheme the *non-cooperative MAC* (NC-MAC).

The second lower bound we consider is a superposition of half-duplex relay channels [4]. Under this model, the third phase of our network in Fig.1 is divided in two new phases. In the new phase 3, node 2 now acts purely as a relay for node 1, whereas in phase 4, node 1 acts purely as a relay for node 2. Phases 1 and 3 thus form a half-duplex relay channel with node 1 as a source, and phases 2 and 4 do the same with node 2. Since we want to treat the more general case, we use the upper bound on the capacity of the half duplex relay channel, and thus write the optimization problem for this lower bound:

$$\begin{array}{ll} \underset{R,\alpha,\mathbf{t}}{\text{min.}} & -R \\ \text{s.t.} & R \le t_1\log\left(1+(1+l_1)\frac{\alpha_1}{t_1}E_{\text{tot}}\right) \\ & \quad + t_3\log\left(1+l_1\frac{v_1}{t_3}E_{\text{tot}}\right) \\ & R \le t_1\log\left(1+l_1\frac{\alpha_1}{t_1}E_{\text{tot}}\right) \\ & \quad + t_3\log\left(1+\left(l_1\alpha_3+l_2\alpha_4+2\sqrt{l_1l_2v_2\alpha_4}\right)\frac{E_{\text{tot}}}{t_3}\right) \\ & R \le t_2\log\left(1+(1+l_2)\frac{\alpha_2}{t_2}E_{\text{tot}}\right) \\ & \quad + t_4\log\left(1+l_2\frac{v_3}{t_4}E_{\text{tot}}\right) \\ & R \le t_2\log\left(1+l_2\frac{\alpha_2}{t_2}E_{\text{tot}}\right) \\ & \quad + t_4\log\left(1+\left(l_1\alpha_6+l_2\alpha_5+2\sqrt{l_1l_2v_4\alpha_6}\right)\frac{E_{\text{tot}}}{t_4}\right) \\ & \mathbb{1}^T\alpha = 1 \\ & \mathbb{1}^T\mathbf{t} = 1 \\ & v_1+v_2=\alpha_3 \\ & v_3+v_4=\alpha_5 \end{array}$$

We call this cooperation scheme *superposed relays* (SR). Like the general problem, we did some variable changes in order to obtain a convex equivalent. We note that the formulation is general enough so that we may consider coherent and non-coherent case for each superposed relay channel in the network.

C. Specific scenarios

We consider these bounds under a number of scenarios for the time and energy allocation. We will denote each of them in the remainder of the paper using Tn/Em to indicate that we refer to the time scenario n and the energy scenario m. As will be shown shortly, most of the realistic cases for these scenarios translate directly into linear equalities for the variables in our optimization problems. Therefore, we can add them freely without breaking the convexity of our formulation [12]. These constraints will use, for the power scenarios, the variables α, β and γ of the superposed relays (SR), the upper bound (UB) and the non-cooperative MAC (NC-MAC) respectively. In a similar manner, constraints for the time scenarios may use the vector τ for the upper bound (UB) problem, and the time vector $\mathbf{t}$ for the superposed relay (SR) problem. At this point, we note that only the original upper bound problem in (4) is the true upper bound on the capacity of the cooperative MAC. If and when a constraint is added to this problem, it only represents the upper bound on the capacity of a *constrained* cooperative MAC, although we still name it the "upper bound problem".

In applications, we may have for the time scenario:

T1) Equal time for each slot in the superposed relay (SR):

$$t_1 = t_2 = t_3 = t_4 \tag{6}$$

The added constraint for the upper bound problem (UB) for this scenario would thus be:

$$\tau_1 = \tau_2 = \frac{1}{2}\tau_3 \tag{7}$$

T2) Arbitrary time sharing between the relays, but fixed separation in half for the subphases of each relay:

$$t_1 = t_3 \qquad t_2 = t_4 \tag{8}$$

Similarly, the upper bound for this scenario would be a relaxation of (7):

$$\tau_1 + \tau_2 = \tau_3 \tag{9}$$

T3) Arbitrary time for each slot, which is the basic formulation of the problems.

These constraints are restricted to the superposed relay case and the upper bound because the non-cooperative MAC case does not use time slots. The energy scenarii are trickier, since problems are rarely defined in terms of energy but rather in terms of power. Nevertheless, we propose de following cases:

E1) Equal energy for each node in each slot in the superposed relay and the upper bound, for each node for the NC-MAC respectively:

$$\alpha_1 = \alpha_2 = \alpha_3 = \alpha_4 = \alpha_5 = \alpha_6 \tag{10}$$
$$\beta_1 = \beta_2 = \beta_3 = \beta_4 \tag{11}$$
$$\gamma_1 = \gamma_2 \tag{12}$$

E2) A more sensible scenario would be to have equal total energy used for each node, once again for SR, UB and NC-MAC respectively:

$$\alpha_1 + \alpha_3 + \alpha_6 = \alpha_2 + \alpha_4 + \alpha_5 \tag{13}$$
$$\beta_1 + \beta_3 = \beta_2 + \beta_4 \tag{14}$$
$$\gamma_1 = \gamma_2 \tag{15}$$

E3) No power used in the second time slot for the source nodes in the SR case. This is to simulate multi-hop transmissions, where the source node would not transmit alongside the relay in the second time slot. This also consequently voids the coherency problem:

$$\alpha_3 = 0 \qquad \alpha_5 = 0 \tag{16}$$

E4) Arbitrary energy for each node in each slot, which reduces to the basic unconstrained problems.

We may also wish for the nodes to limit their peak power in each slot. As it is formulated, we may obtain as a solution to our problem in (4) a nonzero energy sharing term β_i and a very small time sharing term τ_i, which would lead to the transmitted power $\beta_i/\tau_i E_{\rm tot}$ growing to infinity. In practice, we did not encounter such an issue, but we may enforce a maximum power constraint for the nodes. Let's consider for example a constraint $P_{\max}$ on the node A in the slot 1 ; the associated energy sharing term is β_1 and the time sharing term is τ_1 so we would add the inequality constraint:

$$\beta_1 E_{\rm tot} - \tau_1 P_{\max} \leq 0 \tag{17}$$

For the NC-MAC case, this would be equivalent to a maximum energy consumption limit:

$$\gamma_1 E_{\rm tot} - P_{\max} \leq 0 \tag{18}$$

For our problems to retain feasible solutions, we choose to relax the equality constraint on the energy sharing terms to inequalities, allowing the network to consume a fraction of the total energy instead of having the terms sum to 1. In the problem (4) we would thus replace the constraint $\mathbb{1}^T\beta = 1$ by $\mathbb{1}^T\beta \leq 1$.

IV. Results and discussion

Using the scenarii presented in the previous section, we focus here on specific results with interesting consequences in the optimization of cooperative networks.

A. Time and energy scenarii comparison

In realistic cases, it is usually difficult to optimize over every possible parameter of the network, be it the time slot durations or the power values. The scenarii we described thus limit the degrees of freedom of the optimization problem, allowing for a faster and easier solution search. In this first analysis, the results are not necessarily limited to the common rate semi-line. As seen on Fig.2, we represent the upper bound on the capacity region, in order to obtain a fuller view of the impact of the choice of each scenario in the potentially achievable rates of each node.

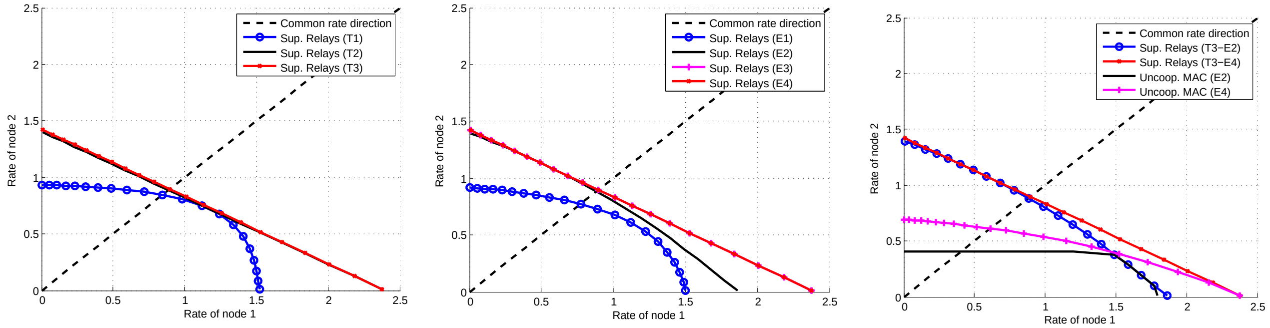

(a) Time scenarii comparison

(b) Energy scenarii comparison

(c) Comparison between cooperative and uncooperative cases

Fig. 2. Comparison between the time and energy scenarii for the superposed relay channels and the uncooperative MAC. The figures represent the upper bound on the capacity region for both nodes in each scenario, with the common rate semi-line crossing the region boundaries. The values used to create these figures were $l_1 = 1$, $l_2 = 0.1$ and $E_{\rm tot} = 10$, meaning that we consider a medium SNR value with one of the source-destination link being of very low quality.

In both the time and energy scenarii – Fig.2a and Fig.2b respectively – we see that the hardest restrictions on the degrees of freedom have a very strong impact. Both the region boundaries for scenarii E1 and T1 are heavily shrinked when compared to the basic formulation of the problems, although we can see that the common rate region $R_1 \approx R_2$ is quite close to the unconstrained boundary. On the other hand, the other scenarii do not impact as much the upper bound on the capacity region. In fact, for example, the scenario T2 in the case we present here gives virtually the same boundary as the unconstrained case. In a similar manner, the scenario E3 gives exactly the same region boundary. This result can be surprising, and in our test is only true when the SNR is relatively low. As $E_{\rm tot}$ increases the difference between the boundaries becomes more apparent.

At last, we compare the cooperative approach of the superposed relay channels with the uncooperative MAC in Fig.2c, under both the E2 and E4 scenarii. The "bad link" hypothesis we use when generating these figures is obviously favouring the cooperative case, especially if we consider the common achievable rate. The uncooperative MAC performs worse in the whole rate region both in the constrained and unconstrained case. In the common rate region $R_1 \approx R_2$ the achievable rate is actually a third of the superposed relay case when we constrain the nodes to each use half of the total energy (scenario E2). On the other hand, as is also seen on Fig.2b, the constraint T3-E2 has virtually no effect near the common rate line for the SR model.

B. Capacity gain through coherency

On Fig.3, we represent the general upper bound on the achievable common rate in the CMAC, in the coherent case. We plot the lower bounds of the superposed relay case in both the coherent case of section III.B and the non-coherent case, which is the same problem with the coherency variables v_1, v_2, v_3 and v_4 set to 0. We aim at characterizing the gain in terms of capacity of going from non-coherent to coherent communications. In order to achieve the maximum performance of the coherent case, there are two main requirements on the communication system ; the first is that both nodes are able to create jointly their codebooks, whereas the second is that both nodes be able to synchronize their respective signals at the destination in order for them to add coherently. The second constraint is the harshest in any wireless network. Indeed, constructing a joint codebook is an easier task if we consider the fact that our nodes operate in a half-duplex fashion.

In the superposed relay case, there is no cooperation between the nodes in the construction of a joint codebook. Indeed, in their respective slot, the nodes do not combine their information and only act either as a pure source or a pure relay. Going from non-coherent relays towards coherent relays thus mainly exploit the potential beamforming gain at the destination. In that light, the results of Fig.3 are clear and the gain of using coherent superposed relays is small, especially when we take into account the inherent complexity of achieving the beamforming. At high SNR, we can also see the uncooperative case crossing the superposed relay, meaning that the latter transmission scheme looses its interest and we should rather optimize the transmission power in the uncooperative MAC.

C. Power limitation at the nodes

The last scenario we propose to analyze in this paper is the case of equations (17) and (18), where the nodes have a peak power constraint that is *a priori* fixed for the whole transmission. We reduce our analysis here to the case where this maximum transmission power $P_{\max}$ is the same for every node in the network, although our formulation can be readily expanded into the case where each node has its own peak power constraint. On Fig.4, we represent the achievable common rate a superposed relay scheme subject to a peak power constraint. The peak constraint is set as a percentage of the total energy constraint – which as an energy constraint over a normalized transmission time of 1 is also a power constraint. As seen on the figure, the peak power constraint has a strong impact on the performances of the network. When this

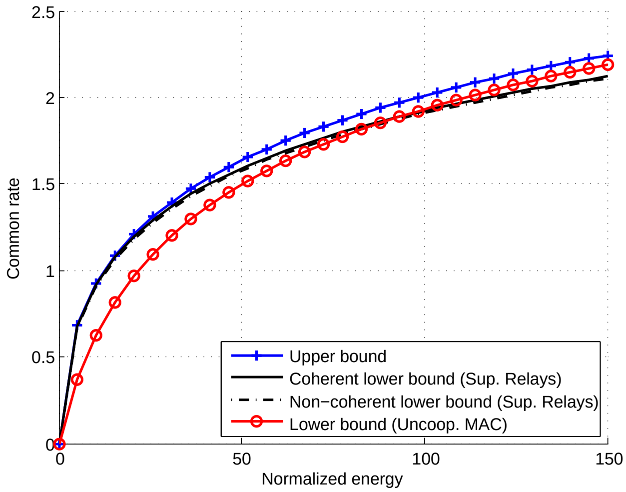

Fig. 3. Bounds on the achievable common rate for the coherent and non-coherent superposed relay. The values used to create these figures were $l_1 = 1$ and $l_2 = 0.1$, the same as in Fig.2. We also plot the achievable rate of the uncooperative case.

constraint prevents the network to allocate the whole of the available energy, the performances are severely degraded. On the other hand, there can be a small drop in performances even though all of the energy is distributed. We can also see that there's a point where the relative value of $P_{\max}$ has no impact on the achievable common rate. At last, the total energy used with respect to the relative value of $P_{\max}$ is linear, and plateaus around $P_{\max} \approx 0.7E_{\text{tot}}$. In our simulations, the plateau point seems to be only dependent on the relative link state and independent of the total available energy E_{tot}.

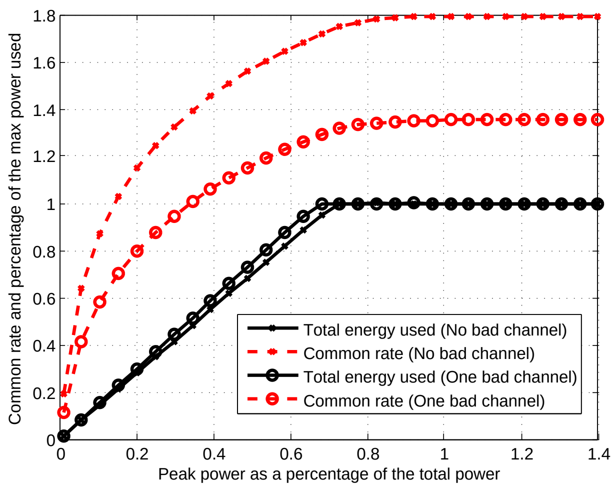

Fig. 4. Achievable common rate through a superposed relay channel cooperation scheme. We represent a "good case" where both the source-destination links are good ($l_1 = l_2 = 1$), and a "bad link case" where like in the previous figures we have $l_1 = 1$ and $l_2 = 0.1$. In both cases the total available energy E_{tot} is set to 30.

V. Conclusion and perspectives

In this paper, we presented an in-depth analysis of the performance of the Gaussian cooperative multiple access channels. We expressed the upper bound and two selected lower bounds on the capacity region as convex optimization problems. This class of problem is hard to solve analytically but there exists efficient solvers giving provably optimal solutions. Since we can readily add linear constraints on the parameters while retaining convex optimization problems, we propose a number of scenarios which reduces the degrees of freedom of the problems. We presented 3 specific cases in order to demonstrate how one may use this framework to answer targeted questions on the capacity of Gaussian CMACs.

Perspectives are numerous ; we showed that some of these scenarios reduce the degrees of freedom of the problems while retaining close performances to the unconstrained case, thus simplifying the analysis. The immediate iteration is to check if the added constraints lead to stronger analytical results. The Gaussian hypothesis should be relaxed and we will consider more realistic fading channels and other metrics that the Shannon capacity. It is expected that cooperative approaches will perform better in fading channels than they do in Gaussian cases, due to the spatial diversity induced by the cooperation between the nodes.

References

[1] G. Kramer, "Models and theory for relay channels with receive constraints," in *42nd Annual Allerton Conf. on Commun., Control, and Computing*, 2004, pp. 1312–1321.

[2] M. Khojastepour, A. Sabharwal, and B. Aazhang, "Bounds on achievable rates for general multi-terminal networks with practical constraints," in *Proceedings of the 2nd international conference on Information processing in sensor networks*. Springer-Verlag, 2003, pp. 146–161.

[3] T. Cover and A. Gamal, "Capacity theorems for the relay channel," *Information Theory, IEEE Transactions on*, vol. 25, no. 5, pp. 572 – 584, sep 1979.

[4] A. Host Madsen and J. Zhang, "Capacity bounds and power allocation for wireless relay channels," *Information Theory, IEEE Transactions on*, vol. 51, no. 6, pp. 2020 –2040, june 2005.

[5] C. Ng and A. Goldsmith, "The impact of CSI and power allocation on relay channel capacity and cooperation strategies," *Wireless Communications, IEEE Transactions on*, vol. 7, no. 12, pp. 5380–5389, December 2008.

[6] F. Parzysz, M. H. Vu, and F. Gagnon, "A half-duplex relay coding scheme optimized for energy efficiency," in *Proc. IEEE Information Theory Workshop (ITW)*, 2011, pp. 306–310.

[7] T. Cover and J. Thomas, *Elements of information theory*, 2nd ed. Springer Verlag, 2006.

[8] J. N. Laneman, "Cooperative Diversity in Wireless Networks: Algorithms and Architectures," Ph.D. dissertation, Massachusetts Institute of Technology, 2002.

[9] A. Sendonaris, E. Erkip, and B. Aazhang, "User cooperation diversity. Part I. System description," *Communications, IEEE Transactions on*, vol. 51, no. 11, pp. 1927 – 1938, nov. 2003.

[10] W. Mesbah and T. N. Davidson, "Optimized Power Allocation for Pairwise Cooperative Multiple Access," vol. 56, no. 7, pp. 2994–3008, 2008.

[11] P. Ferrand, C. Goursaud, and J.-M. Gorce, "Achievable Common Rate and Power Allocation in Cooperative Multiple Access Channels," INSA Lyon, Rapport de recherche, Apr. 2012. [Online]. Available: http://hal.inria.fr/hal-00690407

[12] Stephen Boyd and Lieven Vanderberghe, *Convex Optimization*, Cambridge University Press, Ed. Cambridge University Press, 2007.

[13] Paul T. Boggs and Jon W. Tolle, "Sequential Quadratic Programming," *Acta Numerica*, vol. 4, pp. 1–51, 1995.